Dieses Dokument ist eine Zweitveröffentlichung (Postprint) /

This is a self-archiving document (accepted version):

Min Hyuk Park, Ching-Chang Chung, Tony Schenk, Claudia Richter, Karl Opsomer, Christophe Detavernier, Christoph Adelmann, Jacob L. Jones, Thomas Mikolajick, Uwe Schroeder

Effect of Annealing Ferroelectric HfO2 Thin Films: In Situ, High Temperature X-Ray Diffraction

Erstveröffentlichung in / First published in:

Advanced electronic materials. 2018, 4(7), Art.-Nr. 1800091 [Zugriff am: 24.08.2020]. Wiley. ISSN 2199-160X.

DOI: https://doi.org/10.1002/aelm.201800091

Diese Version ist verfügbar / This version is available on:

https://nbn-resolving.org/urn:nbn:de:bsz:14-qucosa2-804990

SLUB Wir führen Wissen.

TECHNISCHE UNIVERSITÄT DRESDEN

QUCOSA Quality Content of Saxony

Final edited form was published in "Advanced electronic materials". 2018, 4(7), Art.-Nr. 1800091. ISSN 2199-160X.
https://doi.org/10.1002/aelm.201800091

Effect of Annealing Ferroelectric HfO_2 Thin Films: In Situ, High Temperature X-Ray Diffraction

Min Hyuk Park, Ching-Chang Chung, Tony Schenk, Claudia Richter, Karl Opsomer, Christophe Detavernier, Christoph Adelmann, Jacob L. Jones, Thomas Mikolajick, and Uwe Schroeder*

The ferroelectricity in fluorite oxides has gained increasing interest due to its promising properties for multiple applications in semiconductor as well as energy devices. The structural origin of the unexpected ferroelectricity is now believed to be the formation of a non-centrosymmetric orthorhombic phase with the space group of *Pca*2$_1$. However, the factors driving the formation of the ferroelectric phase are still under debate. In this study, to understand the effect of annealing temperature, the crystallization process of doped HfO_2 thin films is analyzed using in situ, high-temperature X-ray diffraction. The change in phase fractions in a multiphase system accompanied with the unit cell volume increase during annealing could be directly observed from X-ray diffraction analyses, and the observations give an information toward understanding the effect of annealing temperature on the structure and electrical properties. A strong coupling between the structure and the electrical properties is reconfirmed from this result.

1. Introduction

The unexpected ferroelectric properties in fluorite-structured binary oxides, such as (doped) HfO_2 and ZrO_2, have gained increasing interest since its first report in 2011.[1,2] Numerous functionalities and devices have been proposed or demonstrated, including ferroelectric random access memory,[3] ferroelectric field effect transistor,[4–6] negative capacitance field effect transistor,[7] pyroelectric energy harvester,[8–11] infrared sensor,[8,9,12] electrocaloric cooler,[7–10] and electrostatic supercapacitor.[13–16] Now it is generally accepted that the origin of this unexpected ferroelectricity is the formation of a noncentrosymmetric orthorhombic phase (o-phase, space group: *Pca*2$_1$).[1,17,18] Sang et al. and Shimizu et al. experimentally confirmed this crystalline phase in doped HfO_2 thin film.[17,18] However, this phase cannot be observed in the phase diagram of bulk HfO_2 and ZrO_2,[19,20] even when doped with elements that are used in the thin film counterparts.[21]

Therefore, multiple factors were suggested as origin of the stabilization of the ferroelectric phase. Materlik et al. suggested that the o-phase can be stabilized due to surface energy effects,[22] and Park et al. comprehensively examined the surface energy model and their experimental observations.[23] In the latter study, it was confirmed that the o-phase can be stabilized within the nuclei formed during the atomic layer deposition (ALD) process, but the interface/grain boundary effect is not sufficient to stabilize the o-phase within the final grain size after annealing.[23] Therefore, it was suggested that the crystalline phase of the initial nuclei can remain even after crystallization, implying that the phase transformation to the monoclinic phase (m-phase, space group: $P2_1/c$) can be kinetically suppressed.[23,24] Stress in thin films was also suggested as a possible origin,[1,25,26] and Shiraishi et al. experimentally proved that the polymorphism of $Hf_{0.5}Zr_{0.5}O_2$ thin films is strongly affected by the thermal expansion coefficient (TEC) of the used substrate.[27] However, the detailed mechanism of the formation of the unexpected o-phase is not yet resolved.

It is generally known that the structure and electrical properties of perovskite ferroelectrics are strongly coupled.[28–30] The ferroelectric properties of doped HfO_2 thin films are also believed to be determined by their crystalline structure. Park

Dr. M. H. Park, Dr. T. Schenk, C. Richter, Prof. T. Mikolajick, Dr. U. Schroeder
NaMLab gGmbH
Noethnitzer Str. 64, 01187 Dresden, Germany
E-mail: MinHyuk.Park@namlab.com

Dr. C.-C. Chung, Prof. J. L. Jones
Department of Materials Science and Engineering
North Carolina State University
Raleigh, NC 27695-7907, USA

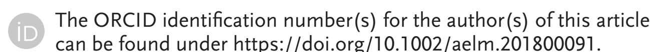
The ORCID identification number(s) for the author(s) of this article can be found under https://doi.org/10.1002/aelm.201800091.

Dr. K. Opsomer, Dr. C. Adelmann
IMEC
B-3001 Leuven, Belgium

Prof. C. Detavernier
Cocoon
Solid State Sciences
Universiteit Gent
B-9000 Gent, Belgium

Prof. T. Mikolajick
Chair of Nanoelectronic Materials
TU Dresden
01062 Dresden, Germany

Provided by Sächsische Landesbibliothek - Staats- und Universitätsbibliothek Dresden

Final edited form was published in "Advanced electronic materials". 2018, 4(7), Art.-Nr. 1800091. ISSN 2199-160X.
https://doi.org/10.1002/aelm.201800091

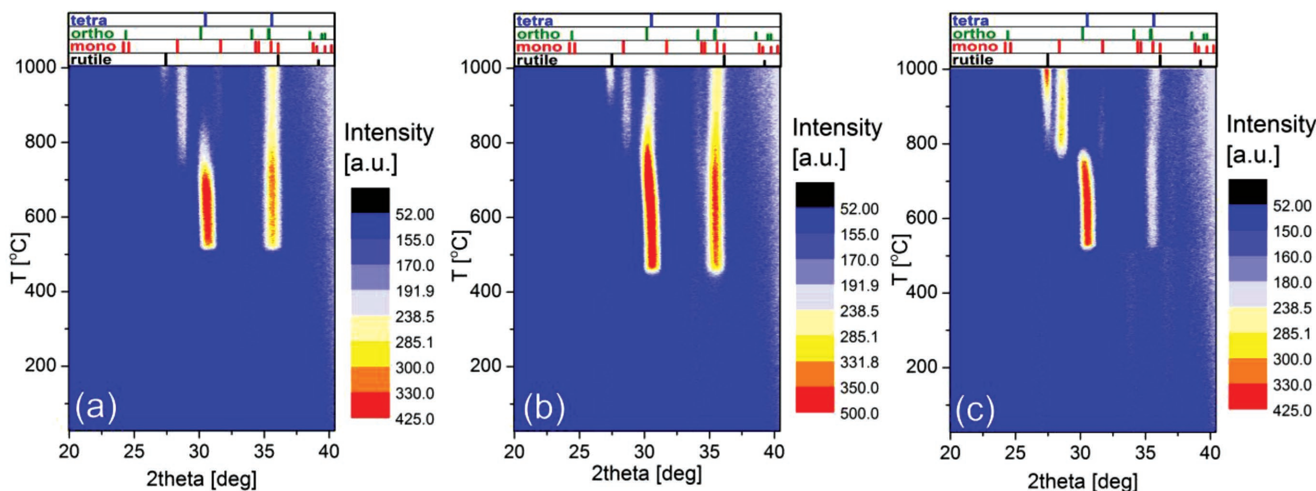

Figure 1. Contour maps constructed from the in situ XRD results from the 10 nm thick a) Al-, b) Gd-, and c) Sr-doped HfO_2 thin films with reference tick marks ($P4_2/nmc$ tetragonal, $Pca2_1$ orthorhombic, $P2_1/c$ monoclinic phases of HfO_2 and $P4_2/mmm$ rutile phase of TiO_2) in the upper panels.

et al. systematically examined the effect of doping concentration on their structure and electrical properties, and reported that they are strongly correlated.[31] Before their work, the structural analysis of the ferroelectric doped HfO_2 thin films using X-ray diffraction (XRD) was considered very difficult, but they found a shift of the o111 or t011 diffraction peak with varying doping concentration.[31] This shift could be related to a change of lattice parameters, aspect ratio (c/a for t-phase and 2a/(b+c) for o-phase), and unit cell volume. For Si-, Al-, and Gd-doped HfO_2 thin films, a similar structural evolution with varying doping concentration could be observed, and they were reasonably linked to the electrical properties.[31] However, in their work, the effect of annealing temperature was not examined although the annealing temperature is another key factor for the ferroelectric properties of doped HfO_2 thin films.[32–36] Moreover, the time dependent crystallization behavior during annealing has not been previously reported. Several previous studies reported the change in XRD patterns at high temperatures, but they focused on the effect of the TiN top electrode on the suppression of the m-phase formation or the effect of doping on the crystallization temperature.[37,38] In this study, therefore, the effect of annealing temperature on the structure and ferroelectric properties of doped HfO_2 thin films is systematically examined. Moreover, the structural evolution during the crystallization process is intensively studied using in situ, high temperature X-ray diffraction.

2. Results and Discussion

2.1. In Situ X-Ray Diffraction

Figure 1a–c shows in situ, high-temperature XRD results represented by contour maps of 10 nm thick Al, Gd, and Sr-doped HfO_2 thin films measured in the temperature range of 30–1000 °C during heating. The patterns measured during cooling are included as given in Figure S1 of the Supporting Information. The doping concentrations of Al-, Gd-, and Sr-doped HfO_2 were 2.8, 1.5, and 4.4 cat%, respectively. The doping concentrations of Al- and Gd-doped HfO_2 were analyzed using time-of-flight secondary ion mass spectrometry (TOF-SIMS), and that of Sr-doped HfO_2 was measured using Rutherford backscattering spectrometry. ALD cycle number ratio between HfO_2 and dopant oxide were 32:1, 27:1, and 39:1 for Al-, Gd-, and Sr-doped HfO_2 thin films, respectively. Films of similar compositions that were annealed at 800 °C for 20 s in the prior work[31] demonstrated robust ferroelectric properties.[35,39,40] The investigated films were amorphous in the as-deposited state, and crystallized during the in situ XRD measurement. From the intensities of the characteristic diffraction peaks in Figure 1a–c the crystallization temperatures of the Al-, Gd-, and Sr-doped HfO_2 thin film were estimated as 515 ± 5, 458 ± 5, and 524 ± 5 °C, respectively. At crystallization temperature, interestingly, metastable phase crystallites (t-phase or o-phase) are first formed. After the initial crystallization, the shift of o111/t011 peak (at ≈30.5°) with varying temperature can be clearly observed for all the three samples. The shift in the o002/o020/t110 peak (at ≈35.5°) was negligible. The detailed shifts of the aforementioned two diffraction peaks are plotted in Figure S2 of the Supporting Information.

In the temperature range between 700 and 800 °C, the m-phase is finally formed for all the films. The phase transition to the m-phase is an irreversible process, and this can be confirmed from the color contour maps for the cooling in Figure S1 of the Supporting Information. It should be noted that the t-phase (or o-phase) to m-phase transition observed in this study is different from the reversible phase transitions typically observed in classical ferroelectrics at the Curie temperature T_c. Once formed, the m-phase does not transform back during subsequent cooling down as shown in Figure S1 of the Supporting Information. Thus, this transition is an irreversible phase transition from the metastable t-phase to the stable m-phase. This point will be further discussed later in this section. In fluorite-type ferroelectrics, the phase transition between the t-phase and o-phase, was experimentally confirmed in Si-doped HfO_2 thin film.[9,41] Typically, a phase transition from the t-phase to the o-phase at T_c is visible. T_c can be lowered from 250 °C for 4 cat% Si to near room temperature (RT) at 7 cat% Si in HfO_2. For Si-doped

Provided by Sächsische Landesbibliothek - Staats- und Universitätsbibliothek Dresden

Final edited form was published in "Advanced electronic materials". 2018, 4(7), Art.-Nr. 1800091. ISSN 2199-160X.
https://doi.org/10.1002/aelm.201800091

HfO_2 the crystallization temperature is higher than T_c. Similar results can be expected for other dopants.

The m-phase formation started at the lowest temperature for Al-doped HfO_2, while it is initiated at the highest temperature for Gd-doped HfO_2. For the case of Sr-doped HfO_2, it seems that the whole film is transformed to the m-phase below 800 °C, while a Gd-doped HfO_2 thin film is not fully transformed to the m-phase even at 1000 °C. The Al-doped HfO_2 film is fully transformed to the m-phase near 900 °C. Since the doping concentration and the chemical properties of the used metal precursors are all different for the three dopants, the observed differences are not necessarily caused by the intrinsic difference between the three dopants. However, it is very interesting that the same trend in structural evolution during in situ XRD study can be observed for the HfO_2 thin film with three different dopants.

Besides the ferroelectric properties, the field-induced-ferroelectric (FFE) phenomenon in doped HfO_2 thin films is also very interesting. It was suggested that the double polarization-electric field hysteresis in Si and Al-doped HfO_2 and for $Hf_{1-x}Zr_xO_2$ thin films originate from the electric field induced phase transition from the t-phase to a polar phase, which can be the o-phase.[8,9,11,37,42] This property is known to be observed in HfO_2 thin films that contain a relatively higher doping concentration compared to the ferroelectric films. To date, strong FFE properties have been reported for $Hf_{1-x}Zr_xO_2$ and Si- or Al-doped HfO_2 thin films,[1,8,9,11,37,42] where the t-phase is known to be formed.[43,44]

For a detailed evaluation, a 40 nm thick 5.7 cat% Si-doped HfO_2 (ALD cycle ration between HfO_2:SiO_2 is 20:1) thin film was chosen to observe the crystallization process of the FFE thin film. Here, thicker films are beneficial to get a high signal to noise ratio from in situ XRD. The doping concentration of Si-doped HfO_2 was analyzed using TOF-SIMS. Recently, Park et al. confirmed a t-phase to o-phase transition with decreasing temperature of a 40 nm thick Si-doped HfO_2 film with the same composition using low temperature (down to ≈−193 °C) in situ XRD measurements.[41] For the analysis of Si-doped HfO_2, a structural evolution during cooling was examined, and in situ XRD which in total consists of four sequences was applied for an in-depth study: 1) First, the sample was heated from RT up to 700 °C to observe the crystallization process. 2) Then, the film was cooled to RT again to examine the effect of thermal contraction during cooling. 3) After that, the film was heated from RT up to 900 °C to observe the volume increase process and the (partial) m-phase formation. 4) Finally, the sample was cooled to RT again.

Figure 2a shows the in situ XRD data acquired using a Bragg–Brentano (BB) geometry from the aforementioned four steps, and Figure 2b depicts the applied temperature as a function of time on the same scale. The overall trend of the m-phase formation and oxidation of the TiN electrode is qualitatively similar to the results from Figure 1. However, the relative intensities of diffraction peaks from the m-phase were lower compared to the results obtained on ferroelectric, doped HfO_2 thin films in Figure S1 of the Supporting Information. This can be understood based on the fact that Si is a strong t-phase stabilizer and that the Si-doped HfO_2 thin film has higher doping concentration compared to the other doped HfO_2 thin films.[43,45]

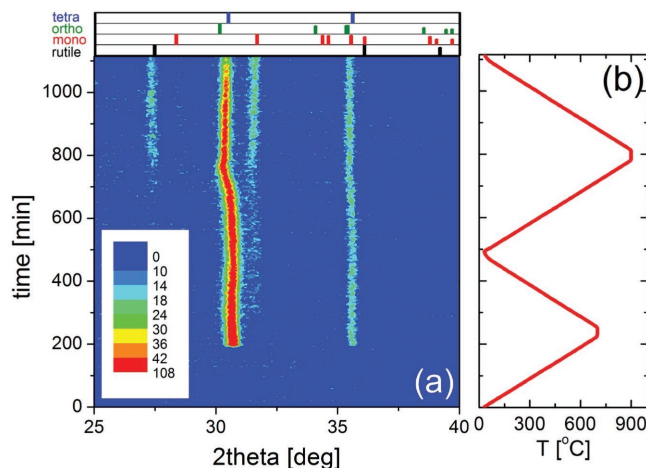

Figure 2. a) In situ, high temperature X-ray diffraction (XRD) results of 40 nm thick Si-doped HfO_2 thin film represented by a contour map with reference patterns ($P4_2/nmc$ tetragonal, $Pca2_1$ orthorhombic, $P2_1/c$ monoclinic phases of HfO_2 and $P4_2/mmm$ rutile phase of TiO_2) in the upper panel. b) Temperature profile applied during the in situ XRD measurement.

From the changes in the peak location in Figure 2a, the aspect ratio and unit cell volume change could be calculated, and summarized in **Figure 3**a,b. The lattice parameters were calculated from interplanar distances d_{111} and d_{002} of o111/t101 peak at ≈30.5° and o002/t110 peak at ≈35° with the assumption that the difference of lattice parameters of two shorter axes is negligible (Figure S3, Supporting Information). The aspect ratio (2a/(b±c) for o-phase and c/a for t-phase) and the unit cell volume (a·b·c) were subsequently determined from the lattice parameters. The details of calculating lattice parameters, aspect ratio and unit cell volume are reported in a previous study.[31]

From the first heating process in Figure 2a, the crystallization started at about 615 °C, and it is higher than T_c reported to be below RT.[44] The crystallization temperature was higher than those of HfO_2 thin films doped with other dopants in Figure 1. It is known that the Si doping increases the crystallization temperature of HfO_2, and Mueller experimentally confirmed this trend in his dissertation.[46,47] With further increasing temperature up to 700 °C during the first step the shift of the o111 diffraction peak is not large, implying negligible structural changes. It is believed that the temperature range for the first heating process is insufficient to induce the phase transition to the m-phase or to increase lattice parameters. During the cooling down to RT within the second step, the shift of the o111 peak is negligible as seen in Figure 2a. There might be a thermal contraction with decreasing temperature, but the magnitude of change is small when the TEC of HfO_2 and Si substrate are considered.[27,48]

The strongest change can be observed during the second heating step up to 900 °C as seen in Figure 2a. When the temperature is higher than about 500 °C, the o111 diffraction peak strongly shifts to lower 2θ values, implying an increase of the unit cell volume. Large changes in the aspect ratio and unit cell volume can be observed in Figure 3a,b. With increasing temperature from 400 to 900 °C, the aspect ratio increases from 1.03 to 1.25, while the unit cell volume increases from to

Provided by Sächsische Landesbibliothek - Staats- und Universitätsbibliothek Dresden

Final edited form was published in "Advanced electronic materials". 2018, 4(7), Art.-Nr. 1800091. ISSN 2199-160X.
https://doi.org/10.1002/aelm.201800091

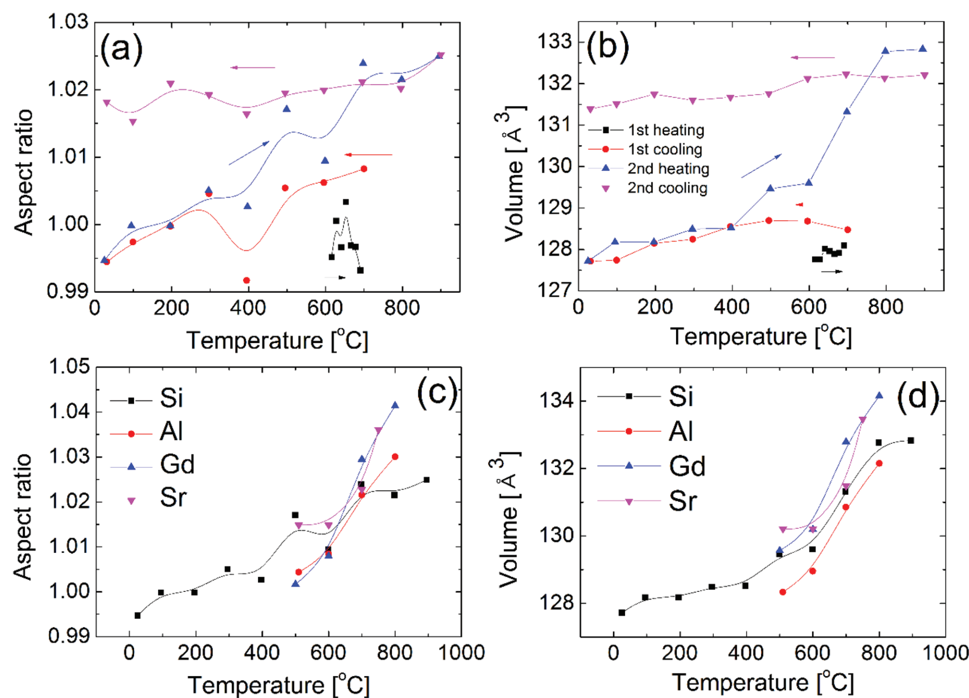

Figure 3. a) Aspect ratio and b) unit cell volume as a function of temperature from the in situ XRD conducted on 40 nm thick Si-doped HfO_2 with four sequences. c) Aspect ratio and d) unit cell volume as a function of temperature for Si-, Al-, Gd-, and Sr-doped HfO_2 thin films.

128.5 to 132.9 Å^3 by 3.4%. This volume increase is beyond the theoretical volume difference (≈2.0%) between the t-phase and the o-phase.[22] The final volume of 132.9 Å^3 is well matched with the theoretical unit cell volume of the o-phase (132.1 Å^3).[22] In addition, the partial phase transformation to the m-phase could also be observed. The theoretical volume difference between the m-phase and the o-phase is 3–4%.[22] On the other hand, during the cool down to RT during the fourth step there were only negligible changes in the aspect ratio and the unit cell volume. It was reported that the upper TiN top electrode can effectively prevent the formation of the m-phase during the cool down process.[1,37,38] In this study, by contrast, a partial formation of the m-phase could be observed despite the high Si doping concentration. We speculate that the relatively low cooling rate used, resulting in a high thermal budget, is the reason for this discrepancy.

Figure 3c,d shows the change of the aspect ratio and the unit cell volume of Si-, Al-, Gd-, and Sr-doped HfO_2 thin films, respectively. For Si-doped HfO_2, the volume change during the second heating was used, since the temperature range for the first heating step was too narrow to observe the strong changes. For all the dopants, interestingly, the aspect ratio and unit cell volume show a similarly increasing trend with increasing temperature. They enhance with increasing temperature. Nevertheless there were some differences between the final values at high temperature before the formation of the m-phase. The final aspect ratio and the unit cell volume of Gd- and Sr-doped HfO_2 thin films were larger than those of Al- and Si-doped HfO_2 thin films. The ionic radius of Gd^{3+} (105 pm) and Sr^{2+} (126 pm) are larger than Hf^{4+} (83 pm) by 26.5 and 51.8%, while those of Al^{3+} (69 pm) and Si^{4+} (54 pm) are smaller by 17.9% and 35.0%.[49,50] The ionic radii for eight-fold coordination were taken or estimated based on extrapolation from a previous study.[49,50] Thus, the different final unit cell volume and the aspect ratio are believed to be strongly related to the ionic radius of the dopants. This result is consistent with our previous study,[40] in which we observed that the unit cell volumes of both the t-phase and the o-phase increase with increasing ionic radius of the dopants.[40]

From the universal trend of increasing aspect ratio and unit cell volume, a general mechanism in the crystallization of doped HfO_2 thin film can be determined. Just beyond the crystallization temperature of doped HfO_2 thin films, we assume that t-phase or c-phase crystallites are formed first. With increasing annealing temperature, the lattice parameters, the aspect ratio, and the unit cell volume increase with increasing temperature. It is generally known that the theoretical aspect ratio of the o-phase (≈1.04) is higher than that of the t-phase (≈1.02) or the c-phase (≈1.00) as confirmed in our previous study.[40] Note that these values are the ones for bulk HfO_2. Therefore, the values of thin films can differ from them. However, it does not necessarily mean that the o-phase exists at such high temperatures. The T_c of doped HfO_2 thin film is believed to be within the temperature range of 400–500 °C.[51] Therefore, the t-phase should exist above T_c, but during cooling after the crystallization process, the t-phase to o-phase transition might occur. The unit cell volume increase should enhance the T_c for doped HfO_2 thin films, since it reduces the strain energy required for the o-phase formation. This phase transition is most likely a martensitic process with a volume increase similar to the phase transition between the t-phase and the o-phase. With further increasing temperature, the o-phase changes to the stable

Provided by Sächsische Landesbibliothek - Staats- und Universitätsbibliothek Dresden

Final edited form was published in "Advanced electronic materials". 2018, 4(7), Art.-Nr. 1800091. ISSN 2199-160X.
https://doi.org/10.1002/aelm.201800091

m-phase. Especially for the case of Sr-doped HfO_2, the whole film transforms to the m-phase at 900 °C. This phase transition to the m-phase is an irreversible process as confirmed from the diffraction patterns analyzed during cooling in Figure S1 of the Supporting Information. The t-phase to m-phase transition has been intensively studied, and is well known that it has a martensitic nature with large volume increase. The activation energy for the martensitic phase transition in ZrO_2 and HfO_2 were reported to be even larger than 200 meV f.u.$^{-1}$.[52,53] Park et al. recently estimated the activation energy for the t-phase to m-phase transition in ferroelectric $Hf_{0.5}Zr_{0.5}O_2$ thin film, and received a value of about 315 meV f.u.$^{-1}$[24]

We now discuss the possible factors involved in the stabilization of the m-phase at elevated temperatures. In the binary phase diagrams of HfO_2-Al_2O_3,[54] HfO_2-Gd_2O_3,[55] HfO_2-SrO,[56] and HfO_2-SiO_2[57] systems, the $Pca2_1$ o-phase cannot be stabilized at any combination of temperature and doping concentration. For the temperature and doping concentration regions examined by the in situ XRD experiments, the m-phase and another secondary phase (α-Al_2O_3, fluorite (Hf,Gd)O_2, perovskite $SrHfO_3$, hafnon $HfSiO_4$ for Al-, Gd-, Sr-, and Si-doped HfO_2, respectively) can be stabilized. Since the entropy of the o-phase or t-phase is higher than that of the m-phase,[22] the o-phase or t-phase should become thermodynamically more favorable with increasing temperature. If the o-phase or t-phase is thermodynamically stabilized, thus, it should not be transformed to the m-phase with increasing temperature. Since the increase in m-phase fraction with increasing temperature cannot be stabilized in doped HfO_2 from the bulk phase diagrams, the other potential factors such as stress, grain size effect, and doping of Ti or N needs to be considered first.

For the ALD of HfO_2 or ZrO_2 thin films, a Volmer–Weber type growth was observed in previous studies,[58–60] and the accordingly expected tensile stress was experimentally confirmed in ferroelectric doped HfO_2 and $Hf_{0.5}Zr_{0.5}O_2$ films.[27,61,62] During the heating phase of the in situ XRD experiment, the tensile strain should decrease since the TEC of the Si substrate is smaller than that of HfO_2. Materlik et al. calculated the free energy of various phases with varying strain, and the free energy of the t-phase or the o-phase decreases with decreasing tensile strain compared to that of the m-phase.[22] A similar trend could be reconfirmed by a comprehensive computational work by Batra et al..[26] These previous studies strongly suggest that a decrease in the m-phase fraction is expected when the tensile stress in doped HfO_2 thin films is released during the heating phase of in situ XRD. This contradicts the experimental observations from in situ XRD.

Based on the interfacial/grain boundary energy effect,[22] grain growth during heating is another potential factor in the phase change from the t-phase or o-phase to the m-phase with increasing temperature. According to Batra et al. report on the surface energy of various phases of HfO_2, the $Pca2_1$ o-phase could not be stabilized with the surface energy effect.[63] Only for a 001-oriented surface the surface energy of the o-phase is lower than that of the m-phase.[63] Instead, the $Pmn2_1$ polar o-phase was energetically more favorable compared to the experimentally observed $Pca2_1$ o-phase.[63] Even worse, the interface and grain boundary energy are much lower than the surface energy.[23] Thus, Batra et al.[26] suggested that various factors including compressive strain and electric field need to be combined to stabilize the $Pca2_1$ o-phase.

Due to high thermal budget during in situ XRD, the effect of diffusion of Ti and N into HfO_2 was also considered as a potential cause for the m-phase formation. However, Ti is known to decrease the t-phase free energy compared to that of the m-phase,[43,45] and Xu et al.[64] showed that N can stabilize o- and t-phase. Thus, the increased fraction of the m-phase cannot be understood based on the diffusion of Ti and N. The 110 diffraction peak from rutile TiO_2 at ≈27.5° starts to appear from 800 to 950 °C (Figure 1), implying a significant chemical change related to intermixing of TiN and doped HfO_2 films. However, the formation of the m-phase starts at temperatures that are a few hundred degrees lower.

From the discussion above, the increasing fraction of the m-phase during heating cannot be explained by changes in the film stress, the grain growth, and the diffusion of Ti and N. This in situ XRD result which shows the m-phase emergence implies that the o-phase or t-phase in HfO_2 might be a metastable phase rather than a thermodynamically stable phase. Instead, the m-phase is the stable phase even for doped HfO_2 thin films similar to bulk HfO_2.

From the kinetic point of view, on the other hand, the increasing thermal energy with increasing temperature can increase the rate of the phase transition when the metastable o- or t-phase is initially formed in doped HfO_2 thin films. Thus, the increasing m-phase fraction with increasing temperature can be attributed to the increasing phase transition rate at higher temperature. The kinetic energy barrier of 315 meV f.u.$^{-1}$ estimated for the o-phase or t-phase to m-phase transition in $Hf_{0.5}Zr_{0.5}O_2$ thin film is about 12 kT (k: Boltzmann constant, T: temperature) at RT. However, the kinetic barrier height is only 3.1 times larger than kT at 900 °C.[24] When it is assumed that the phase transition rate is proportional to $\exp(-E_a/kT)$ where E_a is the kinetic barrier height, the transition rate at 900 °C would be ≈8700 times higher than that at RT. The reason why the metastable o-phase or t-phase nuclei are formed is not clearly elucidated yet. However, the situation for the nucleation in doped HfO_2 thin film can be significantly different from that in bulk HfO_2 due to factors such as local stress field.

2.2. The Effect of Rapid Thermal Process Temperature on the Structure and Electrical Properties

From the in situ XRD results in the previous section, the aspect ratio and unit cell volume of HfO_2 thin films doped with Si, Al, Gd, and Sr increase with increasing temperature during heating. They were considered as a sign of the phase transition from the t-phase to the o-phase. Instead of a low temperature ramp a rapid thermal process (RTP) is also believed to have a similar effect on the structure and electrical properties of doped HfO_2 thin films. In this section, the relation of the crystalline structure to electrical properties of 10 nm thick Si-, Al-, and Gd-doped HfO_2 thin films is examined. It should be noted that the heating and cooling rate of the in situ, XRD measurements and RTP for sample crystallizations are significantly different. Thus, the in situ, XRD results and the effect of RTP temperature for crystallization can be compared only qualitatively.

Provided by Sächsische Landesbibliothek - Staats- und Universitätsbibliothek Dresden

Final edited form was published in "Advanced electronic materials". 2018, 4(7), Art.-Nr. 1800091. ISSN 2199-160X.
https://doi.org/10.1002/aelm.201800091

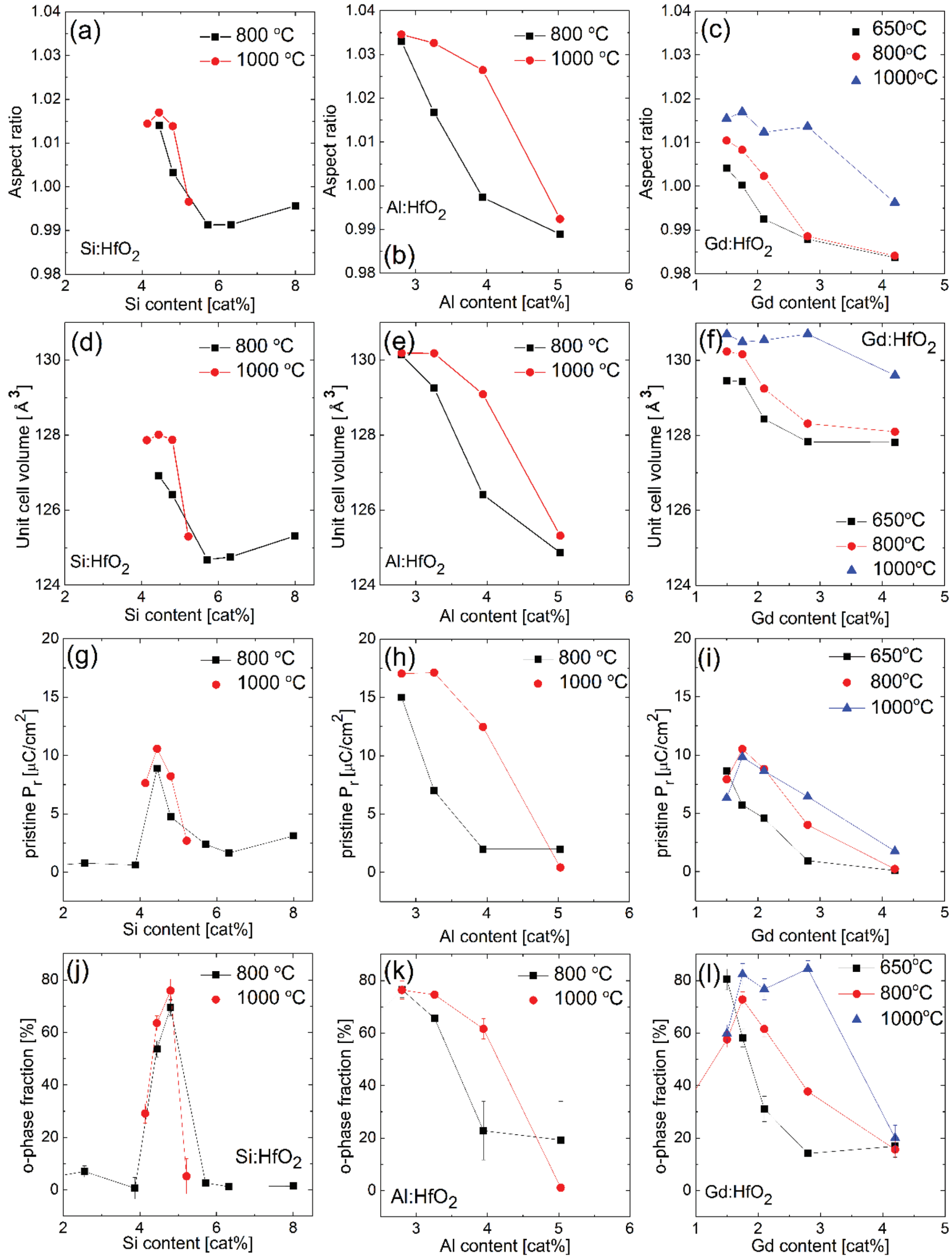

Figure 4. Aspect ratio as a function of doping concentration for a) Si-, b) Al-, and c) Gd-doped HfO_2 thin films. Unit cell volume as a function of doping concentration for d) Si-, e) Al-, and f) Gd-doped HfO_2 thin films. Pristine P_r versus doping concentration for g) Si-, h) Al-, and i) Gd-doped HfO_2 thin films. Orthorhombic phase fraction from Rietveld refinement as functions of doping concentration for j) Si-, k) Al-, and l) Gd-doped HfO_2 thin films.

Figure 4a–c shows the aspect ratio values of Si-, Al-, and Gd-doped HfO_2 thin films annealed at varying temperatures from 650 to 1000 °C. For Si- and Al-doped HfO_2 thin films, the RTP temperature of 800 and 1000 °C were used, while 650, 800, and 1000 °C were used for the Gd-doped HfO_2 thin films. It is believed that Si and Al are stronger stabilizers of the

Provided by Sächsische Landesbibliothek - Staats- und Universitätsbibliothek Dresden

Final edited form was published in "Advanced electronic materials". 2018, 4(7), Art.-Nr. 1800091. ISSN 2199-160X.
https://doi.org/10.1002/aelm.201800091

amorphous phase in HfO_2 compared to Gd.[46,61] The data for the 800 °C annealed samples in Figure 4 were taken from our previous study.[31] Figure 4d–f shows the results on unit cell volumes of Si-, Al-, and Gd-doped HfO_2 thin films. Very interestingly, the aspect ratio and the unit cell volume of all doped HfO_2 films increases with increasing RTP temperature near the doping concentration that yields strong ferroelectricity. Especially, at the composition at the phase boundary between the o-phase and the t-phase the changes in aspect ratio and unit cell volume were the largest among all the studied compositions. The aspect ratio was the largest (up to 1.035) for Al among the dopants, while the unit cell volume was the largest for Gd (up to 131 Å^3).

Figure 4g–i shows the changes in the values of pristine remanent polarization (P_r) for Si-, Al-, and Gd-doped HfO_2 thin films annealed at various temperatures from 650 to 1000 °C. The pristine P_r values were taken instead of the P_r values after wake-up field cycling, since the grazing incidence X-ray diffraction (GIXRD) measurement is conducted for the films before wake-up field cycling. It was suggested that a phase transition can occur during electric field cycling for the wake-up process.[65–68] For the case of pure HfO_2, the P_r is almost zero since the m-phase is dominant. It does not necessarily mean that the undoped HfO_2 cannot be ferroelectric, as reported by several authors.[69,70] With increasing doping concentration to a certain value, the pristine P_r increases due to the increasing o-phase fraction as well as decreasing m-phase fraction. After the maximum P_r value was reached, the P_r decreases with increasing doping concentration due to the phase transition from the o-phase to the t-phase. For the doping concentration conditions for the maximum pristine P_r, the pristine P_r values increase with increasing RTP temperature. The effect of RTP temperature on the pristine P_r value is strongest at the phase boundary between the o-phase and the t-phase. Very interestingly, the change of pristine P_r values is well correlated with the changes in aspect ratio and unit cell volume qualitatively.

To quantitatively examine the crystalline phases in doped HfO_2 films, a Rietveld refinement was conducted. Figure 4j–l shows the determined relative phase fractions of Si-, Al-, and Gd-doped HfO_2 thin films, respectively. Details of the refinement can be found in our previous study.[31] The changes of the o-phase fraction with varying RTP temperature and doping concentration are fairly matched with the changes in pristine P_r values in Figure 4g–i. Although there were differences between the maximum aspect ratio and the maximum unit cell volume between different dopant species, the maximum o-phase fraction does not show strong dopant material dependences. This implies that the pristine P_r values can be affected by other factors as well as the o-phase fraction. It seems that the RTP temperature as well as the dopant species affects the doping concentration range for the o-phase formation.

The effect of dopant species was already discussed in detail in our previous study for the samples annealed at 800 °C.[31] In that paper, it was pointed out that the dopant smaller than Hf tends to stabilize the t-phase since half of the metal-oxygen bonds in the t-phase are shorter than the metal-oxygen bonds in the o-phase.[31] Thus, the t-phase can be stabilized at a relatively lower doping concentration.[31] Batra et al. suggested that the dopants larger than Hf with low electronegativity can better stabilize the o-phase based on their comprehensive computational work.[71] Especially, Gd is one of the dopants which can

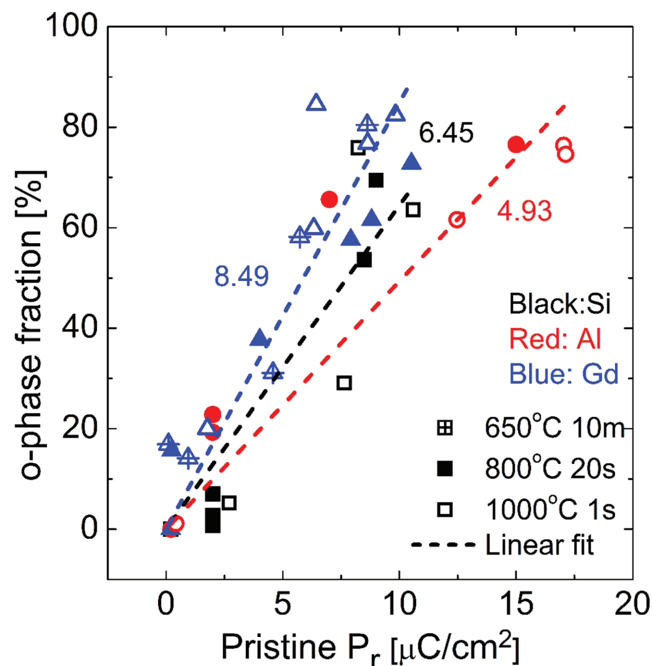

Figure 5. Orthorhombic phase fraction versus pristine P_r plot for Si-, Al-, and Gd-doped hafnium oxide. The lines represent a linear least mean square fit for each dopant. The slopes from the linear fittings are also displayed in the graph.

stabilize the o-phase most effectively.[71] The new finding in this study is that a higher RTP temperature can increase the doping concentration range for the o-phase formation. It seems to be strongly related to the volume increase process during RTP for the crystallization. The unit cell volume of the o-phase is about 1.5–2.0% larger than that of the t-phase. Therefore, the t-phase with larger unit cell parameters formed at higher RTP temperature might easily be transformed to the o-phase during cooling down after RTP. During RTP, the crystalline phase might be the t-phase since temperature is above T_c as reported for Y-doped HfO_2 thin film.[52] Our result implies that the effect of dopant on the crystallization temperature should also strongly affect the formation of the ferroelectric phase. When the HfO_2 thin films are doped with dopants that stabilize the amorphous phase better, a higher RTP temperature might be required to induce the ferroelectric phase. Moreover, the RTP temperature should be carefully controlled to avoid a transformation to the m-phase. Furthermore, it was reported that increasing RTP temperature generally increases the leakage current, and decreases breakdown electric field.[25,33,35,36]

Figure 5 shows the pristine P_r–o-phase fraction plot for all the data included in this study. In our previous study, all the data from the 800 °C annealed Si-, Al-, and Gd-doped HfO_2 could be fitted with a single linear fitting. However, with the dataset from various RTP temperatures, now there is a clear difference visible for the three dopants. Therefore, the data points for each dopants were fitted independently. The expected pristine P_r values for 100% o-phase fraction were 15.5, 20.3, and 11.8 μC cm^{-2}, for Si-, Al-, and Gd-doped HfO_2 thin films, respectively. The calculated P_r values were only 62%, 81%, and 47% of the ideal P_r (≈25 μC cm^{-2}) of a randomly oriented

Provided by Sächsische Landesbibliothek - Staats- und Universitätsbibliothek Dresden

Final edited form was published in "Advanced electronic materials". 2018, 4(7), Art.-Nr. 1800091. ISSN 2199-160X.
https://doi.org/10.1002/aelm.201800091

orthorhombic HfO_2 thin film.[22,72] It should be noted that the pristine P_r values can be affected by various factors, so the different relation between pristine P_r and o-phase fraction cannot be considered as an intrinsic properties of the dopants. For the case of Gd-doped HfO_2 thin films, Hoffmann et al. reported P_r up to 18 μC cm^{-2} with top and bottom TiN electrode, and this could increase even up to 35 μC cm^{-2} with top and bottom TaN electrodes.[35] To understand the intrinsic effect of dopants on the ferroelectric properties of the doped HfO_2 thin films, further studies are still required.

The observation from the doped HfO_2 thin films with various doping concentration and RTP temperatures is well-matched with the observation from in situ XRD. From the in situ XRD, the aspect ratio and the unit cell volume of doped HfO_2 increase with increasing temperature, and it was the same for the doped HfO_2 thin films annealed at various temperatures. However, the temperature range for the strong change was higher for the RTP temperature experiment compared to the in situ XRD observation. This discrepancy is believed to be a consequence of the slow heating rate of in situ XRD. However, a qualitatively consistent trend with varying temperature suggests that the RTP temperature effect can be understood based on the observations from the in situ XRD. The same crystalline structural evolution with varying aspect ratio and unit cell volume should occur during the RTP.

The results in this paper are also well-matched with the previous reports on the effect of RTP temperature on the ferroelectric properties of doped HfO_2 thin films. Park et al. reported that the o-phase fraction in $Hf_{0.5}Zr_{0.5}O_2$ thin films increased with increasing RTP temperature from 400 to 600 °C directly related to the increase in P_r values.[25] With further increasing RTP temperature up to 800 °C, the m-phase fraction enhances with decreasing P_r,[25] and this trend is consistent with our observations in doped HfO_2 thin films. Yurchuk et al. also reported that the P_r of Si-doped HfO_2 thin film increases with increasing RTP temperature from 650 to 1000 °C.[32] In their report, it seems that 1000 °C was even not sufficient to induce the phase transition to the m-phase.[32] Hoffmann et al. also reported that P_r of Gd-doped HfO_2 thin film improved with increasing RTP temperature.[35] However, in their studies, the changes in the structural evolutions have not been carefully examined.[35] Therefore, the in situ XRD results and a comprehensive study of the effect of RTP temperature on the structure and electrical characteristics can deepen the understanding ferroelectric properties in fluorite oxide thin films.

3. Conclusion

In conclusion, the crystallization process of ferroelectric or field induced ferroelectric doped HfO_2 thin films were comprehensively studied using in situ XRD measurements. From the results, the crystallization process can be summarized consisting of the following three steps. 1) First, crystallites having a tetragonal or cubic crystalline structure are formed. 2) With increasing temperature the lattice parameters increase similar to those of the o-phase. This most likely results in the increase of T_c and the formation of the o-phase during cooling down. 3) Finaly a stable m-phase is formed at high temperature. From our observation, it is very likely that the ferroelectric o-phase in doped HfO_2 thin films is a metastable phase rather than a thermodynamically stable phase. This conclusion is consistent with the phase stability expected in bulk materials. As expected from the in situ XRD, the aspect ratio and the unit cell volume increase with increasing RTP temperature, and this effect was the strongest for the composition close to the phase boundary between the orthorhombic and the tetragonal phase. The strong coupling between the structure and electrical properties could be confirmed for the two important parameters doping concentration and RTP temperature.

4. Experimental Section

Thin, doped HfO_2 films were deposited by an ALD on TiN electrodes on p-type 100 Si substrates. The TiN bottom electrode was deposited via reactive sputtering at RT using a Ti target within a nitrogen (N_2) atmosphere for Si- and Al-doped HfO_2 films, and via plasma enhanced ALD for Gd-doped HfO_2 films. For the deposition of Si-doped HfO_2 films, tetrakis(ethylmethylamino)hafnium (TEMAHf) and *N*,*N*,*N′*,*N′*-tetraethyl silanediamine (SAM.24) were used as Hf and Si precursors, and water and oxygen plasma were used as oxygen sources, respectively. The doping concentration within films could be controlled by changing the ALD cycle ratio of HfO_2 versus dopant oxide. For the deposition of Al-doped HfO_2 films, $HfCl_4$, and $Al(CH_3)_3$ (TMA) were used as precursors, respectively, and water was used as an oxidant both for Hf and Al. The wafer temperature during ALD process was 300 °C. For the deposition of Gd-doped HfO_2 films, hafnium $HfCl_4$ and $Gd(iPrCp)_3$ were used as precursors, and water was used as an oxidant both for Hf and Gd. For the case of Sr-doped HfO_2 films, $HfCl_4$, and $Sr(tBu_3Cp)_2$ were used as precursors while H_2O was used for an oxygen source. The experimental details of the ALD processes can be found in the previous studies.[33,35,39,40] On the deposited HfO_2 films, a TiN top electrode was deposited using reactive sputtering using a Ti target within a N_2 atmosphere. For capacitor samples utilized for electrical characterization, a RTP was conducted at 650 °C for 10 min, 800 °C for 20 s, or 1000 °C for 1 s in N_2 atmosphere for the crystallization of the films using an AST rapid thermal processing tool. For the case of the Si-doped HfO_2 thin films annealed at 1000 °C, the films were subsequently annealed at 650 °C for 20 s after the annealing at 1000 °C for 1 s. However, the effect of subsequent annealing at much lower temperature on the crystalline structure should be negligible. After the RTP process, Pt electrodes were deposited via e-beam evaporation through a shadow mask during the evaporation process. Patterned Pt top electrodes were used as a hard mask during the subsequent TiN wet etch process using a standard clean 1 solution containing NH_4OH, H_2O_2, and water.

Ferroelectric properties were analyzed by a ferroelectric tester (TF analyzer 3000, Aixacct systems). A triangular bipolar waveform was applied to the top electrode while the bottom electrode was connected to the virtual ground within a measurement frequency range of 1–10 kHz. The P_r values for doped HfO_2 films were taken from the polarization–electric field curves achieved with 4.0 MV cm^{-1} pulse height. The P_r values in pristine states were compared to structural data for a comparison.

The evolution of the crystalline structures of the 10 nm thick Al-, Gd-, and Sr-doped HfO_2 thin films was monitored as a function of temperature by in situ XRD. At a fixed 2θ window, every 5 s a diffraction spectrum is acquired using a position sensitive detector while the sample is heated at a constant heating rate of 0.2 °C s^{-1} from room temperature to 1000 °C in a 250 sccm He flow. After reaching the maximum temperature, the sample is subjected to free cooling in the same He flow, while diffraction patterns are acquired down to 70 °C every 5 s.

The crystal structure of a 40 nm thick Si-doped HfO_2 film was analyzed using an X-ray diffractometer (Empyrean, PANalytical)

Provided by Sächsische Landesbibliothek - Staats- und Universitätsbibliothek Dresden

Final edited form was published in "Advanced electronic materials". 2018, 4(7), Art.-Nr. 1800091. ISSN 2199-160X. https://doi.org/10.1002/aelm.201800091

with a high temperature chamber (HTK1200, Anton Paar) in N_2 atmosphere. Two thermal cycles were applied to the sample during the measurement. In the first cycle, the sample was heated in the chamber from 25 to 700 °C with a heating rate of 3 °C min^{-1}, held at 700 °C for 30 min. After that, the sample was cooled to 25 °C with a cooling rate of 3 °C min^{-1}. In the second cycle, the sample was reheated up to 900 °C with a heating rate of 3 °C min^{-1} and held at 900 °C for 30 min before cooling to 25 °C. Diffraction patterns were measured throughout the whole heat treatment using Cu Kα X-ray radiation with a wavelength of 1.5418 Å and a 2θ range of 25–40°. Each pattern was measured for 4 min using a 2θ step size and integration time of 0.0263° and 33 s per step, respectively.

The crystalline structure of Si-, Al-, and Gd-doped HfO_2 thin films was analyzed using an X-ray diffractometer (D8 Discover, Bruker) within grazing incidence geometry. Here, the incidence angle was fixed at 0.45°, and the diffraction patterns were analyzed within a 2θ range of 15–90°. The TiN top electrode was etched before the GIXRD measurement. For the quantitative phase analysis, a commercial software for Rietveld refinement (TOPAS, Bruker) was used. A detailed description of the Rietveld refinement can be found in the previous study.[40]

Supporting Information

Supporting Information is available from the Wiley Online Library or from the author.

Acknowledgements

The authors gratefully acknowledge the support of the Army Research Office through Contract No. W911NF-15-1-0593. M.H.P. was supported by Humboldt postdoctoral fellowship by Alexander von Humboldt foundation. T.S. gratefully acknowledges the German Research Foundation (Deutsche Forschungsgemeinschaft) for funding part of this research in the frame of the "Inferox" project (MI 1247/11-2). This work was performed in part at the Analytical Instrumentation Facility (AIF) at North Carolina State University, which is supported by the State of North Carolina and the National Science Foundation (Award No. ECCS-1542015). The AIF is a member of the North Carolina Research Triangle Nanotechnology Network (RTNN), a site in the National Nanotechnology Coordinated Infrastructure (NNCI).

Conflict of Interest

The authors declare no conflict of interest.

Keywords

ferroelectricity, fluorite structure, hafnia, phase transitions, X-ray diffraction

Received: February 13, 2018
Revised: March 27, 2018
Published online: May 16, 2018

[1] T. S. Böscke, J. Müller, D. Bräuhaus, U. Schröder, U. Böttger, *Appl. Phys. Lett.* **2011**, *99*, 102903.
[2] M. H. Park, Y. H. Lee, H. J. Kim, Y. J. Kim, T. Moon, K. D. Kim, J. Müller, A. Kersch, U. Schroeder, T. Mikolajick, C. S. Hwang, *Adv. Mater.* **2015**, *27*, 1811.
[3] S. Mueller, S. R. Summerfelt, J. Müller, U. Schroeder, T. Mikolajick, *IEEE Electron Device Lett.* **2012**, *33*, 1300.
[4] J. Müller, E. Yurchuk, J. Paul, R. Hoffmann, S. Müller, D. Martin, S. Slesazeck, P. Polakowski, J. Sundqvist, M. Czernohorsky, K. Seidel, P. Kücher, R. Boschke, M. Trentzsch, K. Gebauer, U. Schröder, T. Mikolajick, *Symp. on VLSI Technology Digest of Technical Papers*, IEEE, Piscataway, NJ **2012**, p. 25, https://doi.org/10.1109/VLSIT.2012.6242443.
[5] J. Müller, T. S. Böscke, Y. Yurchuk, P. Polakowski, J. Paul, D. Martin, T. Schenk, K. Khullar, A. Kersch, W. Weinreich, S. Riedel, K. Seidel, A. Kumar, T. M. Arruda, S. V. Kalinin, T. Schlosser, R. Boschke, R. van Bentum, U. Schröder, T. Mikolajick, *IEEE Int. Electron Devices Meet.*, IEEE, Piscataway, NJ **2013**, p. 10.8.1, https://doi.org/10.1109/IEDM.2013.6724605.
[6] H. Yu, C.-C. Chung, N. Shewmon, S. Ho, J. H. Carpenter, R. Larrabee, T. Sun, J. L. Jones, H. Ade, B. T. O'Connor, F. So, *Adv. Funct. Mater.* **2017**, *27*, 1700461.
[7] M. Hoffmann, M. Pešić, K. Chatterjee, A. I. Khan, S. Salahuddin, S. Slesazeck, U. Schroeder, T. Mikolajick, *Adv. Funct. Mater.* **2016**, *26*, 8643.
[8] M. H. Park, H. J. Kim, Y. J. Kim, T. Moon, K. D. Kim, C. S. Hwang, *Nano Energy* **2015**, *12*, 131.
[9] M. Hoffmann, U. Schroeder, C. Künneth, A. Kersch, S. Starschich, U. Böttger, T. Mikolajick, *Nano Energy* **2015**, *18*, 154.
[10] M. H. Park, H. J. Kim, Y. J. Kim, T. Moon, K. D. Kim, Y. H. Lee, S. D. Hyun, C. S. Hwang, *Adv. Mater.* **2016**, *28*, 7956.
[11] M. H. Park, T. Schenk, M. Hoffmann, S. Knebel, J. Gartner, T. Mikolajick, U. Schroeder, *Nano Energy* **2017**, *36*, 381.
[12] S. W. Smith, A. R. Kitahara, M. A. Rodriguez, M. D. Henry, M. T. Brumbach, J. F. Ihlefeld, *Appl. Phys. Lett.* **2017**, *110*, 072901.
[13] M. H. Park, H. J. Kim, Y. J. Kim, T. Moon, K. D. Kim, C. S. Hwang, *Adv. Energy Mater.* **2014**, *4*, 201400610.
[14] M. Pešić, M. Hoffmann, C. Richter, T. Mikolajick, U. Schroeder, *Adv. Funct. Mater.* **2016**, *26*, 7486.
[15] P. D. Lomenzo, C.-C. Chung, C. Zhou, J. L. Jones, T. Nishida, *Appl. Phys. Lett.* **2017**, *110*, 232904.
[16] K. D. Kim, Y. H. Lee, T. Gwon, Y. J. Kim, H. J. Kim, T. Moon, S. D. Hyun, H. W. Park, M. H. Park, C. S. Hwang, *Nano Energy* **2017**, *39*, 390.
[17] X. Sang, E. D. Grimley, T. Schenk, U. Schroeder, J. M. LeBeau, *Appl. Phys. Lett.* **2015**, *106*, 162905.
[18] T. Shimizu, K. Katayama, T. Kiguchi, A. Akama, T. J. Konno, H. Funakubo, *Appl. Phys. Lett.* **2015**, *107*, 032910.
[19] O. Ohtaka, H. fukui, T. Kunisada, T. Fujisawa, K. Funakoshi, W. Utsumi, T. Irifune, K. Kuroda, T. Kikegawa, *J. Am. Ceram. Soc.* **2001**, *84*, 1369.
[20] O. Ohtaka, H. fukui, T. Kunisada, T. Fujisawa, K. Funakoshi, W. Utsumi, T. Irifune, K. Kuroda, T. Kikegawa, *Phys. Rev. B* **2001**, *63*, 174108.
[21] L. Zhao, M. Nelson, H. Aldridge, T. Iamsasri, C. M. Fancher, J. S. Forrester, T. Nishida, S. Moghaddam, J. L. Jones, *J. Appl. Phys.* **2014**, *115*, 034104.
[22] R. Materlik, C. Künneth, A. Kersch, *J. Appl. Phys.* **2015**, *117*, 134109.
[23] M. H. Park, Y. H. Lee, H. J. Kim, T. Schenk, W. Lee, K. D. Kim, F. P. G. Fengler, T. Mikolajick, U. Schroeder, C. S. Hwang, *Nanoscale* **2017**, *9*, 9973.
[24] M. H. Park, Y. H. Lee, H. J. Kim, Y. J. Kim, K. D. Kim, S. D. Hyun, T. Mikolajick, U. Schroeder, C. S. Hwang, *Nanoscale* **2018**, *10*, 716.
[25] M. H. Park, H. J. Kim, Y. J. Kim, W. Lee, T. Moon, C. S. Hwang, *Appl. Phys. Lett.* **2013**, *102*, 242905.
[26] R. Batra, T. D. Huan, J. L. Jones, G. Rossetti Jr., R. Ramprasad, *J. Phys. Chem. C* **2017**, *121*, 4139.
[27] T. Shiraishi, K. Katayama, T. Yokouchi, T. Shimizu, T. Oikawa, O. Sakata, H. Uchida, Y. Imai, T. Kiguchi, T. J. Konno, H. Funakubo, *Appl. Phys. Lett.* **2016**, *108*, 262904.
[28] D. G. Schlom, L.-Q. Chen, C.-B. Eom, K. M. Rabe, S. K. Streiffer, J.-M. Triscone, *Annu. Rev. Mater. Res.* **2007**, *37*, 589.

Provided by Sächsische Landesbibliothek - Staats- und Universitätsbibliothek Dresden

Final edited form was published in "Advanced electronic materials". 2018, 4(7), Art.-Nr. 1800091. ISSN 2199-160X.
https://doi.org/10.1002/aelm.201800091

[29] C. Ederer, N. A. Spaldin, *Phys. Rev. Lett.* **2005**, *95*, 257601.
[30] J. H. Haeni, P. Irvin, W. Chang, R. Uecker, P. Reiche, Y. L. Li, S. Choudhury, W. Tian, M. E. Hawley, B. Craigo, A. K. Tagantsev, X. Q. Pan, S. K. Streiffer, L. Q. Chen, S. W. Kirchoefer, J. Levy, D. G. Schlom, *Nature* **2004**, *430*, 758.
[31] M. H. Park, T. Schenk, C. M. Fancher, E. D. Grimley, C. Zhou, C. Richter, J. M. LeBeau, J. L. Jones, T. Mikolajick, U. Schroeder, *J. Mater. Chem. C* **2017**, *5*, 4677.
[32] E. Yurchuk, J. Müller, S. Knebel, J. Sundqvist, A. P. Graham, T. Melde, U. Schröder, T. Mikolajick, *Thin Solid Films* **2013**, *533*, 88.
[33] C. Richter, T. Schenk, M. H. Park, F. A. Tscharntke, E. D. Grimley, J. M. LeBeau, C. Zhou, C. M. Fancher, J. L. Jones, T. Mikolajick, U. Schroeder, *Adv. Electron. Mater.* **2017**, *3*, 1700131.
[34] M. H. Park, H. J. Kim, Y. J. Kim, T. Moon, K. D. Kim, C. S. Hwang, *Phys. Status Solidi RRL* **2014**, *8*, 857.
[35] M. Hoffmann, U. Schroeder, T. Schenk, T. Shimizu, H. Funakubo, O. Sakata, D. Pohl, M. Drescher, C. Adelmann, R. Materlik, A. Kersch, T. Mikolajick, *J. Appl. Phys.* **2015**, *118*, 072006.
[36] T. Mittmann, F. P. G. Fengler, C. Richter, M. H. Park, T. Mikolajick, U. Schroeder, *Microelectron. Eng.* **2017**, *178*, 48.
[37] J. Müller, T. S. Böscke, U. Schröder, S. Mueller, D. Bräuhaus, U. Böttger, L. Frey, T. Mikolajick, *Nano Lett.* **2012**, *12*, 4318.
[38] J. Müller, U Schröder, T. S. Böscke, I. Müller, U. Böttger, L. Wilde, J. Sundqvist, M. Lemberger, P. Kücher, T. Mikolajick, L. Frey, *J. Appl. Phys.* **2011**, *110*, 114113.
[39] T. Schenk, S. Mueller, U. Schroeder, R. Materlik, A. Kersch, M. Popovici, C. Adelmann, S. Van Elshocht, T. Mikolajick, *2013 Proc. of the European Solid-State Device Research Conf. (ESSDERC), Bucharest*, IEEE, Piscataway, NJ **2013**, pp. 260–263, https://doi.org/10.1109/ESSDERC.2013.6818868.
[40] M. H. Park, T. Schenk, C. M. Fancher, E. D. Grimley, C. Zhou, C. Richter, J. M. LeBeau, J. L Jones, T. Mikolajick, U. Schroeder, *J. Mater Chem. C* **2017**, *5*, 4677.
[41] M. H. Park, H. J. Kim, Y. H. Lee, Y. J. Kim, T. Moon, K. D. Kim, S. D. Hyun, C. S. Hwang, *Nanoscale* **2016**, *8*, 13898.
[42] C.-K. Lee, E. Cho, H.-S. Lee, C. S. Hwang, S. Han, *Phys. Rev. B* **2008**, *78*, 012102.
[43] U. Schroeder, E. Yurchuk, J. Müller, D. Martin, T. Schenk, P. Polakowski, C. Adelmann, M. I. Popovici, S. V. Kalinin, T. Mikolajick, *Jpn. J. Appl. Phys.* **2014**, *53*, 08LE02.
[44] M. H. Park, C.-C. Chung, T. Schenk, C. Richter, M. Hoffmann, S. Wirth, J. L. Jones, T. Mikolajick, U. Schroeder, *Adv. Electron. Mater.* **2018**, *4*, 1700489.
[45] D. Cunningham, *Ph.D. Thesis*, University of Connecticut, USA **2014**.
[46] J. Müller, *Ph.D. Thesis*, TU Dresden, Germany **2014**.
[47] C. Fachmann, L. Frey, S. Kudelka, T. Boescke, S. Nawka, E. Erben, T. Doll, *Microelectron. Eng.* **2007**, *84*, 2883.
[48] R. P. Haggerty, P. Sarin, Z. D. Apostolov, P. E. Driemeyer, W. M. Kriven, *J. Am. Ceram. Soc.* **2014**, *97*, 2213.
[49] R. D. Shannon, *Acta. Crystallogr.* **1976**, *A32*, 751.
[50] G. S. Rohrer, *Structure and Bonding in Crystalline Materials*. The Press Syndicate of the University of Cambridge, Cambridge, UK **2004**.
[51] T. Shimizu, K. Katayama, T. Kiguchi, A. Akama, T. J. Konno, O. Sakata, H. Funakubo, *Sci. Rep.* **2016**, *6*, 32931.
[52] X. Luo, W. Zhou, S. V. Ushakov, A. Navrotsky, A. A. Demkov, *Phys. Rev. B* **2009**, *80*, 134119.
[53] B. M. Hudak, S. W. Depner, G. R. Waetzig, A. Talapatra, R. Arroyave, S. Banerjee, B. S. Guiton, *Nat. Commun.* **2017**, *8*, 15316.
[54] L. M. Lopato, A. V. Shevchenko, G. I. Gerasimyuk, *Izv. Akad. Nauk SSSR Neorg. Mater.* **1976**, *12*, 1623; *Inorg. Mater. (Eng. Transl.)* **1976**, *12*, 1331.
[55] A. V. Shevchenko, L. M. Lopato, *Inorg. Mater.* **1982**, *18*, 1583.
[56] A. V. Shevchenko, L. M. Lopato, A. I. Stegnii, A. K. Ruban, V. S. Dvernyakov, V. V. Pasnichnyi, *Inorg. Mater.* **1981**, *17*, 741.
[57] V. N. Parfenenkov, R.G. Grebenshikov, N.A. Toropov, *Dokl. Akad. Nauk SSSR* **1969**, *185*, 840.
[58] M. L. Green, A. J. Allen, X. Li, J. Wang, J. Ilavsky, A. Delabie, R. L. Puurunen, B. Brijs, *Appl. Phys. Lett.* **2006**, *88*, 032907.
[59] W. F. A. Besling, E. Young, T. Conard, C. Zhao, R. Carter, W. Vandervorst, M. Caymax, S. De Gendt, M. Heyns, J. Maes, M. Tuominen, S. Haukka, *J. Non-Cryst. Solids* **2002**, *303*, 123.
[60] E. P. Gusev, C. Cabral, M. Copel, C. D'Emic, M. Gribelyuk, *Microelectron. Eng.* **2003**, *69*, 145.
[61] T. Schenk, *Ph.D. Thesis*, TU Dresden, Germany **2016**.
[62] U. Schroeder, C. Richter, M. H. Park, T. Schenk, M. Pešić, M. Hoffmann, F. P. G. Fengler, D. Pohl, B. Rellinghaus, C. Zhou, C. C. Chung, J. L. Jones, T. Mikolajick, *Inorg. Chem.* **2018**, *57*, 2752.
[63] R. Batra, H. D. Huan, R. Ramprasad, *Appl. Phys. Lett.* **2016**, *108*, 172902.
[64] L. Xu, T. Nishimura, S. Shibayama, T. Yajima, S. Migita, A. Toriumi, *Appl. Phys. Express* **2016**, *9*, 091501.
[65] P. D. Lomenzo, Q. Takmeel, C. Zhou, C. M. Fancher, E. Lambers, N. G. Rudawski, J. L. Jones, S. Moghaddam, T. Nishida, *J. Appl. Phys.* **2015**, *117*, 134105.
[66] H. J. Kim, M. H. Park, Y. J. Kim, Y. H. Lee, T. Moon, K. D. Kim, S. D. Hyun, C. S. Hwang, *Nanoscale* **2016**, *8*, 1383.
[67] M. Pešić, F. P. G. Fengler, L. Larcher, A. Padovani, T. Schenk, E. D. Grimley, X. Sang, J. M. LeBeau, S. Slesazeck, U. Schroeder, T. Mikolajick, *Adv. Funct. Mater.* **2016**, *26*, 4601.
[68] M. H. Park, H. J. Kim, Y. J. Kim, Y. H. Lee, T. Moon, K. D. Kim, S. D. Hyun, F. Fengler, U. Schroeder, C. S. Hwang, *ACS Appl. Mater. Interfaces* **2016**, *8*, 15466.
[69] P. Polakowski, J. Müller, *Appl. Phys. Lett.* **2015**, *106*, 232905.
[70] K. D. Kim, M. H. Park, H. J. Kim, Y. J. Kim, T. Moon, Y. H. Lee, S. D. Hyun, T. Gwon, C. S. Hwang, *J. Mater. Chem. C* **2016**, *4*, 6864.
[71] R. Batra, T. D. Huan, G. A. Rossetti Jr., R. Ramprasad, *Chem. Mater.* **2017**, *29*, 9102.
[72] J. L. Jones, *Mater. Sci. Eng. B* **2016**, *167*, 6.

Provided by Sächsische Landesbibliothek - Staats- und Universitätsbibliothek Dresden